Cluster radioactivity preformation probability of trans-lead nuclei in the N_pN_n scheme

Lin-Jing Qi,[1] Dong-Meng Zhang,[1] Song Luo,[1] Gui-Qing Zhang [●],[2,*] Peng-Cheng Chu [●],[3,†]
Xi-Jun Wu,[4,‡] and Xiao-Hua Li [●][1,5,6,§]

[1]*School of Nuclear Science and Technology, University of South China, 421001 Hengyang, People's Republic of China*
[2]*College of Science, University of Science and Technology, 300457 Tianjin, People's Republic of China*
[3]*The Research Center for Theoretical Physics, Science School,*
Qingdao University of Technology, Qingdao 266033, People's Republic of China
[4]*School of Math and Physics, University of South China, Hengyang 421001, People's Republic of China*
[5]*Cooperative Innovation Center for Nuclear Fuel Cycle Technology and Equipment,*
University of South China, 421001 Hengyang, People's Republic of China
[6]*National Exemplary Base for International Science and Technology Collaboration of Nuclear Energy and Nuclear Safety,*
University of South China, Hengyang 421001, People's Republic of China

In the present work, the cluster radioactivity preformation probability P_c in the scheme of N_pN_n for the effective number of the valence particles (holes) in trans-lead nuclei has been systematically investigated. This quantity has been explored in the simplified parametrization of N_pN_n as well as the multiplication N_pN_nI of this product with the isospin asymmetry I. The calculations for P_c are both performed in microscopic and model-dependent way. Within the microscopic approach, based on our previous work [Chin. Phys. C **47**, 014101 (2023)], P_c is calculated in cluster formation model combined with the exponential relationship of P_c to the α decay preformation probability P_α when the mass number of the emitted cluster $A_c \leqslant 28$. While $A_c \geqslant 28$, P_c is obtained through the charge-number dependence of P_c on the decay products proposed by Ren *et al.* [Phys. Rev. C **70**, 034304 (2004)]. In the model-dependent approach, P_c is extracted through the ratios from calculated cluster radioactivity half-lives in the framework of unified fission model proposed by Dong *et al.* [Eur. Phys. J. A **41**, 197 (2009)] to experimental ones. Both of the results show P_c in logarithmic form are linear to N_pN_n as well as N_pN_nI. For comparison, the parent-mass-number dependence analytical formula as well as the model proposed by Wei and Zhang [Phys. Rev. C **96**, 021601(R) (2017)] are also used. Furthermore, the preformation mechanic for cluster radioactivity has also been discussed.

I. INTRODUCTION

Nuclear physics was originated from the discovery of natural radioactivity. Nuclear spontaneous disintegration has always been the effective probe for investigating nuclear structure. In 1980, Săndulescu, Poenaru, and Greiner primarily predicted a novel spontaneous emission phenomenon in unstable nuclei whose emitted fragments, heavier than α particles but less than fission fragments, generally are known as cluster radioactivity [1–5]. Soon afterwards, this decay mode was experimentally confirmed by Rose and Jones through observing ^{14}C particle emitted from a ^{223}Ra isotope [6–9]. Since then, an increasing number of clusters heavier than a ^{14}C particle such as ^{20}O, ^{23}F, $^{22,24–26}$Ne, ^{28,30}Mg, and ^{32,34}Si isotopes are availably observed on experiments in the parent nuclei ranging from ^{221}Fr up to ^{242}Cm in trans-lead region decaying to the doubly magic nucleus ^{208}Pb or its neighboring nuclei

[10–13], further providing a unique way to explore various nuclear structures.

Since cluster radioactivity, proton radioactivity, two-proton radioactivity, and α decay are similarly explained as the quantum mechanical effect [14–24], in particular, due to the immediate characteristic between α decay and spontaneous fission, there are generally two kinds of theoretical methods within Gamow's theory well established to interpret this rare decay mode: α-like models and fission-like models [25]. Furthermore, the cluster radioactivity preformation probability is dealt with differently in these two models [4,26–28]. In α-like models, the cluster is assumed to already be preborn in the parent nuclei with certain probability before penetrating the interacting barrier between the emitted cluster and the daughter nucleus [29–32]. For actually, in density-dependent cluster model (DDCM) proposed by Ren *et al.*, the cluster preformation probability is assumed as an exponential function as the multiplication of the emitted cluster charge number as well as daughter charge number employed to calculate the half-lives of cluster radioactivity [33,34]. In preformed cluster model (PCM), it is obtained by solving the stationary Schrödinger equation for the dynamical flow of mass and charge [35]. However, in fission-like models, cluster radioactivity

———————
*nkzhanggq@tust.edu.cn
†kyois@126.com
‡wuxijunusc@163.com
§lixiaohuaphysics@126.com

preformation probability is regarded as the penetration probability of the pre-scission part for the interacting barrier [36,37]. For instance, in Coulomb and proximity potential (CPPM) proposed by Santhosh *et al.* [38], the cluster formation probability is calculated as the penetrability probability through the internal part of the potential barrier through the simple power-law interpolation.

Noticeably, P_c plays an indispensable incorporated part in calculating cluster radioactivity half-lives [39]. Moreover, it is an important indicator possessing abundant information of nuclear structure such as shell effects, surface deformation and neutron-proton (n-p) interaction in our previous study and investigation from other researchers [40–43]. Since cluster radioactivity is closely related to shell effects and P_c can be considered as the penetrability for the overlapping region between the actual ground state configuration of the parent and the configuration described by the emitted cluster coupled to the ground state of the daughter nucleus [44], the tunneling probability of the emitted cluster is expected to be significantly dependent on the n-p interaction. Various quantities, such as deformation, ground band energy systematics, and properties of excited states, can be parametrized in the scheme of $N_p N_n$ or obtained through the simple functions of N_p and/or N_n which may also bear smooth relationships with the observables [45]. The n-p interaction can be well represented by these parametrization and simple functions [45,46]. Previous work has indicated the general behavior of P_c in logarithmic form linearly decreases with the neutron number arriving at a local minimum as the magic shell closures and then linearly increase again [41]. This phenomenon may imply P_c exhibits a certain correlation when it is expressed as a function of the product of N_p and N_n. In the present work, we make attempts to explore the relationship of cluster radioactivity preformation probability versus valence nucleons (holes) in the scheme of $N_p N_n$, while cluster radioactivity preformation probability is calculated both microscopically and model-dependently. In the microscopic approach, based on our previous work, the cluster radioactivity preformation probability is dealt with cluster formation model (CFM) combined with the exponential relationship of P_c to the α decay preformation probability P_α when the number of the emitted cluster $A_c \leqslant 28$. It should be noted that, as is clearly indicated in Fig. 2 from Ref. [42], P_c in logarithmical form keeps a good linear relationship with the mass number of the emitted cluster. The curve is bent obviously when $A_c > 28$ and the slope of the curve begin to decrease with the increasing of the emitted cluster mass number. Therefore, in the present work, while $A_c \geqslant 28$, P_c is obtained through the charge-number dependence of P_c on the decay products proposed by Ren *et al.* [33]. In the model-dependent approach, P_c is extracted through the ratios from the calculated cluster radioactivity half-lives to experimental ones, while the cluster radioactivity half-lives calculations are preformed in the unified fission model (UFM) [47].

This article is organized as follows. A brief introduction of the theoretical framework for the UFM and CFM is briefly presented in Sec. II. Detailed numerical results and discussion are given in Sec. III. Section IV is a simple summary.

II. THEORETICAL FRAMEWORK

A. Model-dependent approach

In UFM, for the emitted cluster-daughter system, the barrier penetration probability P can be obtained by the Wentzel-Kramers-Brillouin (WKB) approximation action integral [47]

$$P = \exp\left\{-\frac{2}{\hbar}\int_{R_{in}}^{R_{out}}\sqrt{2\mu(V(r)-Q_c)}dr\right\}, \quad (1)$$

where $\hbar$ is the reduced Planck constant and $\mu = \frac{M_c M_d}{M_c + M_d}$ is the reduced mass of emitted cluster-daughter nucleus system with M_c and M_d being the masses of emitted cluster and daughter nucleus, respectively [48]. Q_c is the cluster radioactivity decay energy. It can be obtained by [49]

$$Q_c = B(A_c, Z_c) + B(A_d, Z_d) - B(A, Z), \quad (2)$$

where $B(A_c, Z_c)$, $B(A_d, Z_d)$, and $B(A, Z)$ are, respectively, the binding energy of the emitted cluster, daughter and parent nuclei taken from AME2020 [50] and NUBASE2020 [51]. A_c, Z_c, A_d, Z_d, and A, Z are the mass numbers and proton numbers of the emitted cluster, daughter, and parent nucleus, respectively. $R_{in} = R_1 + R_2$ and $R_{out} = \frac{Z_c Z_d e^2}{2Q_c} + \sqrt{(\frac{Z_c Z_d e^2}{2Q_c})^2 + \frac{l(l+1)\hbar^2}{2\mu Q_c}}$ are the radius for the separation configuration and the outer turning point [47] with R_1 and R_2 being the equivalent sharp radii of the daughter nucleus and the emitted cluster, respectively. They can be obtained by [49]

$$R_i = (1.28 A_i^{1/3} - 0.76 + 0.8 A_i^{-1/3})\text{fm}, i = 1, 2. \quad (3)$$

The total interacting potential $V(r)$ between the emitted cluster and daughter nucleus consists of the repulsive long-range Coulomb potential $V_C(r)$, the attractive short-range nuclear proximity potential V_p, and the centrifugal potential $V_l(r)$ when the fragments are separated. It is expressed as [47]

$$V(r) = V_p(r) + V_C(r) + V_l(r), \quad (4)$$

where r is the distance between the fragment centers. The inclusion of the proximity potential reduces the height of the barrier which closely agrees with the experimental values. The nuclear proximity potential takes the following form [47]:

$$V_p(r) = 4\pi \frac{C_1 C_2}{C_1 + C_2} \gamma b \Phi(s), \quad (5)$$

where the Süsmann central radii $C_i = R_i - \frac{b^2}{R_i}$ with $b = 0.99$ fm being the surface width. The nuclear surface tension coefficient γ is given as [27]

$$\gamma = 0.9517[1 - 1.7826\left(\frac{N-Z}{A}\right)^2]\text{MeV fm}^{-2}, \quad (6)$$

where N represents the neutron number of the parent nucleus. The universal function $\Phi(s)$ is parametrized as [27]

$$\Phi(s) = \begin{cases} \frac{1}{2}(s-2.54)^2 - 0.00852(s-2.54)^3, & s \leqslant 1.2511, \\ -3.437 \exp\left(-\frac{s}{0.75}\right), & s \geqslant 1.2511, \end{cases} \quad (7)$$

where $s = (r - C_1 - C_2)/b$ is the overlap distance in units of b for the colliding surfaces.

The Coulomb potential in Eq. (4) is given as [40]

$$V_C(r) = \frac{e^2 Z_c Z_d}{r^2}, \tag{8}$$

where $e^2 = 1.4399652 \, \text{MeV fm}$ is the square of the electronic elementary charge [40]. As for the centrifugal potential $V_l(r)$, since $l(l+1) \to (l+\frac{1}{2})^2$ is a necessary correction for one-dimensional problems [52], we choose it as the Langer modified form in this work. It can be expressed as

$$V_l(r) = \frac{\hbar^2 \left(l + \frac{1}{2}\right)^2}{2\mu r^2}, \tag{9}$$

where l is the angular momentum carried by the emitted cluster. It can be obtained by [53]

$$l = \begin{cases} \Delta_j, & \text{for even } \Delta_j \text{ and } \pi_p = \pi_d, \\ \Delta_j + 1, & \text{for even } \Delta_j \text{ and } \pi_p \neq \pi_d, \\ \Delta_j, & \text{for odd } \Delta_j \text{ and } \pi_p \neq \pi_d, \\ \Delta_j + 1, & \text{for odd } \Delta_j \text{ and } \pi_p = \pi_d, \end{cases} \tag{10}$$

where $\Delta_j = |j_p - j_d - j_c|$, j_c, π_c, j_p, π_p, and j_d, π_d are the isospin and parity values of the emitted cluster, parent, and daughter nuclei, respectively.

The assault frequency ν_0 is calculated by [47]

$$\nu_0 = \frac{1}{R_0} \sqrt{\frac{2E_k}{M}}, \tag{11}$$

where $E_k = \frac{A - A_c}{A} Q_c$ and M are the kinetic energy and mass of the emitted cluster, respectively. R_0 is the equivalent sharp radius of the parent nucleus. With the experimental cluster radioactivity half-life, the preformation probability can be extracted from [47]

$$P_c = \frac{\ln 2}{T_{\exp} \nu_0 P}. \tag{12}$$

B. Microscopic approach

Within the framework of CFM, the total initial clusterization state ψ of the emitted cluster-daughter nucleus system is considered as a linear superposition of all its n possible clusterization ψ_i states [54]. It can be expressed as

$$\psi = \sum_i^N a_i \psi_i, \tag{13}$$

$$a_i = \int \psi_i^* \psi \, d\tau, \tag{14}$$

where a_i represents the superposition coefficient of ψ_i which satisfies the orthogonality condition [55]

$$\sum_i^N |a_i|^2 = 1. \tag{15}$$

Correspondingly, the total Hamiltonian H consists of the Hamiltonian H_i for different clusterization configuration ψ_i which can be expressed as [56]

$$H = \sum_i^N H_i. \tag{16}$$

By virtue of all the clusterization states describing the same emitted cluster-daughter nucleus system, they are assumed as sharing the same total eigenenergy E of the total wave function [57]. Furthermore, considering the orthogonality of the clusterization wave functions, E can be expressed as

$$E = \sum_i^N |a_i|^2 E = \sum_i^N E_{f_i}, \tag{17}$$

where E_{f_i} represents the formation energy for the cluster in the i-th clusterization state ψ_i. For α decay, the preformation probability P_α can be obtained by [56]

$$P_\alpha = |a_\alpha|^2 = \frac{E_{f_\alpha}}{E}. \tag{18}$$

Here, a_α and E_{f_α} are the coefficient of the α clusterization state and the formation energy of the α particle, respectively.

Moreover, the α formation energy E_{f_α} and total system energy E can be classified as four different cases in the following expressions [53].

Case *I* for even-even nuclei:

$$E_{f_\alpha} = 3B(A, Z) + B(A - 4, Z - 2)$$
$$- 2B(A - 1, Z - 1) - 2B(A - 1, Z), \tag{19}$$

$$E = B(A, Z) - B(A - 4, Z - 2). \tag{20}$$

Case *II* for even-odd nuclei:

$$E_{f_\alpha} = 3B(A - 1, Z) + B(A - 5, Z - 2)$$
$$- 2B(A - 2, Z - 1) - 2B(A - 2, Z), \tag{21}$$

$$E = B(A, Z) - B(A - 5, Z - 2). \tag{22}$$

Case *III* for odd-even nuclei:

$$E_{f_\alpha} = 3B(A - 1, Z - 1) + B(A - 5, Z - 3)$$
$$- 2B(A - 2, Z - 2) - 2B(A - 2, Z - 1), \tag{23}$$

$$E = B(A, Z) - B(A - 5, Z - 3). \tag{24}$$

Case *IV* for odd-odd nuclei:

$$E_{f_\alpha} = 3B(A - 2, Z - 1) + B(A - 6, Z - 3)$$
$$- 2B(A - 3, Z - 2) - 2B(A - 3, Z - 1), \tag{25}$$

$$E = B(A, Z) - B(A - 6, Z - 3). \tag{26}$$

When $A_c < 28$, P_c in logarithmic form keeps a good linear relationship with P_α. Using this relation, P_c can be obtained by [58]

$$P_c = [P_\alpha]^{\frac{(A_c - 1)}{3}}. \tag{27}$$

As for $A_c > 28$, the calculations for the P_c are completed by a formula proposed by Ren *et al.* [33] for this law may not work. It can be expressed as

$$\log_{10} P_c = \begin{cases} -(0.01674 Z_c Z_d - 2.035466), \\ \quad \text{for even-even nuclei,} \\ -(0.01674 Z_c Z_d - 2.035466) - 1.175, \\ \quad \text{for odd-}A \text{ nuclei.} \end{cases} \tag{28}$$

TABLE I. Cluster radioactivity preformation probability in microscopic and model-dependent approaches. See text for details.

decay	Q_c(MeV)	$T_{1/2}^{\exp}$	N_p	N_n	I	CFM	UFM
^{221}Fr $\rightarrow$ ^{207}Tl + ^{14}C	31.29	14.56	5	8	0.213	-3.204	-6.420
^{221}Ra $\rightarrow$ ^{207}Pb + ^{14}C	32.40	13.39	6	7	0.204	-3.126	-6.388
^{222}Ra $\rightarrow$ ^{208}Pb + ^{14}C	33.05	11.22	6	8	0.207	-3.037	-5.547
^{223}Ra $\rightarrow$ ^{209}Pb + ^{14}C	31.83	15.05	6	9	0.211	-3.440	-7.160
^{224}Ra $\rightarrow$ ^{210}Pb + ^{14}C	30.53	15.87	6	10	0.214	-3.186	-5.593
^{226}Ra $\rightarrow$ ^{212}Pb + ^{14}C	28.20	21.2	6	12	0.221	-3.211	-6.014
^{223}Ac $\rightarrow$ ^{209}Bi + ^{14}C	33.06	12.6	8	12	0.202	-3.341	-6.060
^{228}Th $\rightarrow$ ^{208}Pb + ^{20}O	44.72	20.73	8	12	0.211	-4.670	-8.174
^{231}Pa $\rightarrow$ ^{208}Pb + ^{23}F	51.88	26.02	9	14	0.212	-5.999	-12.495
^{230}Th $\rightarrow$ ^{206}Hg + ^{24}Ne	57.76	24.63	8	14	0.217	-5.661	-11.349
^{231}Pa $\rightarrow$ ^{207}Tl + ^{24}Ne	60.41	22.89	9	14	0.214	-6.271	-12.074
^{232}U $\rightarrow$ ^{208}Pb + ^{24}Ne	62.31	20.39	10	14	0.207	-5.924	-11.195
^{233}U $\rightarrow$ ^{209}Pb + ^{24}Ne	60.49	24.84	10	15	0.210	-6.672	-13.145
^{234}U $\rightarrow$ ^{210}Pb + ^{24}Ne	58.82	25.93	10	16	0.214	-6.313	-11.904
^{233}U $\rightarrow$ ^{208}Pb + ^{25}Ne	60.70	24.84	10	15	0.210	-6.962	-13.126
^{234}U $\rightarrow$ ^{208}Pb + ^{26}Ne	59.41	25.93	10	16	0.214	-6.862	-12.074
^{234}U $\rightarrow$ ^{206}Hg + ^{28}Mg	74.11	25.53	10	16	0.214	-7.411	-13.928
^{236}Pu $\rightarrow$ ^{208}Pb + ^{28}Mg	79.67	21.52	12	16	0.203	-7.689	-14.132
^{238}Pu $\rightarrow$ ^{210}Pb + ^{28}Mg	75.91	25.7	12	18	0.210	-7.547	-13.903
^{238}Pu $\rightarrow$ ^{208}Pb + ^{30}Mg	76.79	25.7	12	18	0.210	-9.452	-14.561
^{238}Pu $\rightarrow$ ^{206}Hg + ^{32}Si	91.19	25.28	12	18	0.210	-11.039	-15.625
^{242}Cm $\rightarrow$ ^{208}Pb + ^{34}Si	96.54	23.15	14	20	0.207	-11.366	-16.511

III. RESULTS AND DISCUSSION

The aim of this work is to systematically investigate the behavior of cluster radioactivity preformation probability of trans-lead nuclei in the scheme of $N_p N_n$. Numerous researchers have discovered such dependence in α decay. For instance, the works of Seif *et al.* reported that α decay preformation probability of even-even nuclei around the $Z = 82$, $N = 126$ closed shells linearly depend on the product of the valance protons (holes) and neutrons (holes) $N_p N_n$ [59,60]. Furthermore, in our previous works, we systematically studied the P_α of the favored and unfavored α decay for odd-A and doubly odd nuclei, where P_α is extracted from the ratios of calculated α decay half-lives to experimental values [24,61]. The results indicated that P_α is linearly to $N_p N_n$ although it is model dependent. Before long, Deng *et al.* further pointed out that this linear relationship simultaneously satisfies all types of nuclei well in α decay [62]. For α decay and cluster radioactivity share the same physical mechanism, it is interesting to explore whether it is a possibility for the cluster radioactivity preformation probability to have certain correlation with the product of valance protons (holes) and neutrons (holes) $N_p N_n$. For further verifying this assumption, in the present work, we use two different approaches to deal with preformation probability of cluster radioactivity. In UFM, P_c is usually treated as unity. Theoretically, it can be extracted by the ratios from the calculated cluster radioactivity half-lives to experimental ones. Using this method, the cluster radioactivity preformation probability is deduced model-dependently. To this end, based on our previous work, when the mass number of the emitted cluster $A_c \leqslant 28$, we calculate the preformation penetrability of cluster radioactivity through the famous exponential law of P_c to the α decay

preformation probability P_α, while P_α is obtained within microcosmic model CFM. Whereas $A_c \geqslant 28$, the preformation factor can be obtained through the charge-number dependence of P_c on the decay products proposed by Ren *et al.* [33]. A detailed discussion about the later approach has been given in Ref. [40]. Both the calculated results are well listed in Table I. In this table, the first to third columns represent the decay process, cluster radioactivity decay energies, and experimental cluster radioactivity half-lives in logarithmic form taken from Refs. [38,52] denoted as decay, Q_c and $T_{1/2}^{\exp}$, respectively. The effective number of valence protons and neutrons for the parent nucleus expressed as $N_p = Z - Z_0$ and $N_n = N - N_0$ are presented in fourth and fifth columns denoted as N_p and N_n with Z_0 and N_0 being the nearest proton and neutron closed shells, respectively. In this work, we choose ($Z_0 = 82$, $N_0 = 126$) as the considered doubly magic core for the cluster radioactivity whose decaying daughter nucleus are around the doubly magic nucleus ^{208}Pb or its neighboring nuclei in trans-lead region. Then N_p and N_n can be obtained by $N_p = Z - 82$ and $N_n = N - 126$. The sixth column represents the isospin asymmetry of the parent nuclei $I = (N - Z)/(N + Z)$. The seventh and eighth columns represent the cluster radioactivity preformation factor deduced from microscopic and model-dependent approaches in logarithmic form denoted as CFM and UFM, respectively. From this table, it is obviously to see that the cluster radioactivity preformation probability P_c values even for the order of magnitude are comparably different obtained by using above two methods while the tendency of the individual variations for P_c values are basically consistent. The results have indicated that exploring the cluster radioactivity preformation probability in both model-dependent and microscopic way is of necessity. It is well acknowledged that conventional counting of valence protons and neutrons can
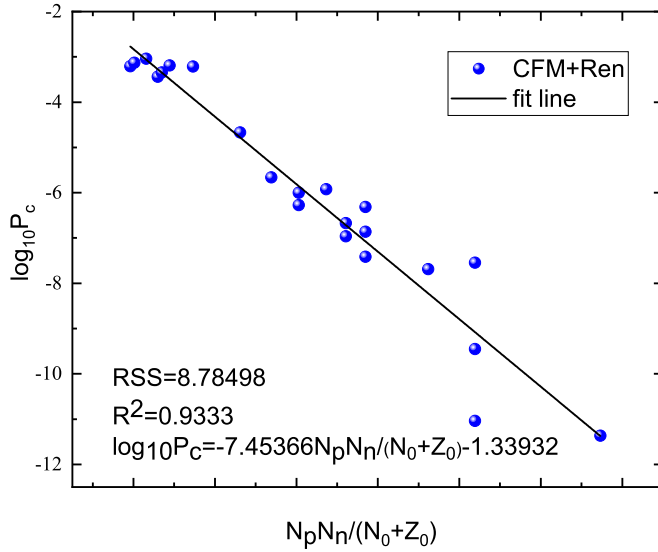
FIG. 1. The linear relationship of the cluster radioactivity preformation probability in logarithmic form by using microscopic approach with the product of the valance protons (holes) and neutrons (holes) N_pN_n.

be inadequate on account of change in magic number and shell structure in diverse mass regions [45]. Making use of effective number of valence particles in the N_pN_n scheme may significantly improve the predictability of the scheme as well as point to the emergence of new shell structure in various mass regions. In that regard, in order to have an intuitive insight to the dependence for P_c along with valence particles (holes), the correlation between P_c in logarithmic form obtained through UFM as well as CFM with valence particles (holes) in the form of $\frac{N_pN_n}{N_0+Z_0}$ are plotted in Figs. 1 and 2. As can
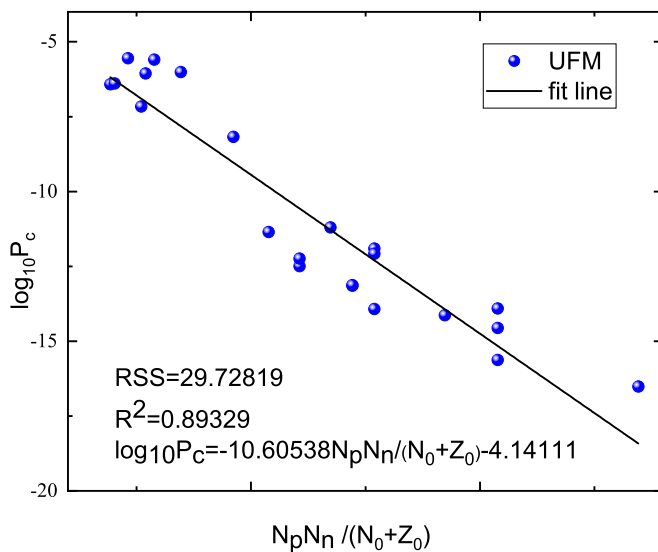

FIG. 2. The linear relationship of the cluster radioactivity preformation probability in logarithmic form by using model-dependent approach with the product of the valance protons (holes) and neutrons (holes) N_pN_n.
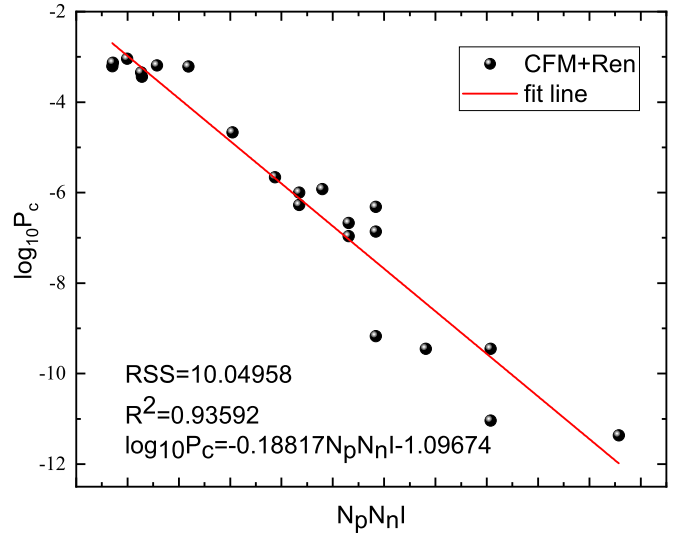

FIG. 3. The linear relationship of the cluster radioactivity preformation probability obtained by microscopic approach in logarithmic form versus the quantity N_pN_nI.

be clearly seen from these two pictures, P_c in logarithmic form are similarly varying smoothly and have linear relationships with the products of the number of the valence protons and neutrons. It can be expressed as

$$\log_{10}P_c = a\frac{N_pN_n}{N_0+Z_0} + b, \tag{29}$$

where a and b are the adjustable parameters extracted from the fittings of Figs. 1 and 2.

Moreover, we introduce the statistical quantities, the minimum residual sum of squares (RSS) which represents the sum of squares due to error as well as the coefficient of determination R^2, to estimate the degree of fitting. In the present work, RSS can be defined as

$$\text{RSS} = \sum \left(\log_{10}T_{1/2}^{\text{calc}} - \log_{10}\hat{T}_{1/2}^{\text{calc}}\right)^2, \tag{30}$$

where $\log_{10}T_{1/2}^{\text{calc}}$ and $\log_{10}\hat{T}_{1/2}^{\text{calc}}$ are the logarithmic form of calculated cluster radioactivity half-lives and the value for the corresponding spot on the regression straight line. The total sum of squares (TSS) can be obtained by

$$\text{TSS} = \sum \left(\log_{10}T_{1/2}^{\text{calc}} - \log_{10}\bar{T}_{1/2}^{\text{calc}}\right)^2, \tag{31}$$

where $\log_{10}\bar{T}_{1/2}^{\text{calc}}$ denotes the average value for the logarithmic form of calculated cluster radioactivity half-lives. To this end, the coefficient of determination R^2 can be expressed as

$$R^2 = \frac{\text{TSS} - \text{RSS}}{\text{TSS}} = 1 - \frac{\text{RSS}}{\text{TSS}}. \tag{32}$$

The smaller the value of RSS and the larger the value of R^2 approaching 1, the better the degree of fit. a and b are fitted with the minimum RSS and $R^2 \approx 1$. The detailed corresponding values of a, b, RSS, and R^2 are given in Figs. 1 and 2.
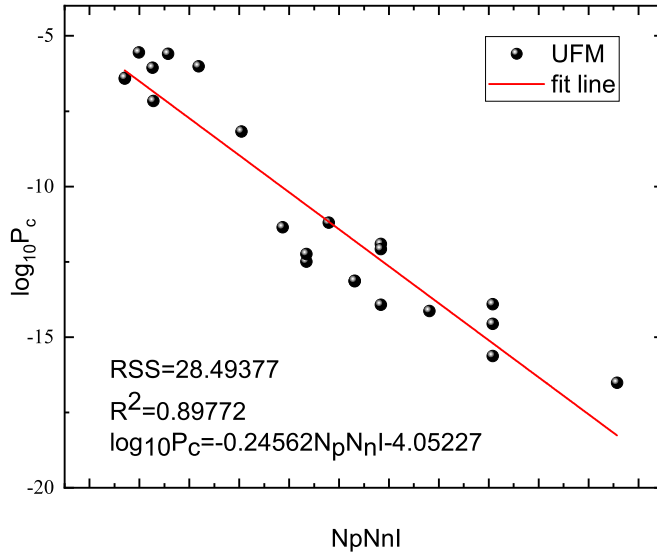
FIG. 4. The linear relationship of the cluster radioactivity preformation probability obtained by model-dependent approach in logarithmic form versus the quantity $N_p N_n I$.

The general behavior of P_c in logarithmic form shows a decrease with the increase of $N_p N_n$. Furthermore, for the value of parent nucleus isospin asymmetry depends on the doubly magic core at (N_0, Z_0), we size up the P_c by incorporating the isospin asymmetry into $N_p N_n$, which can be expressed as

$$\log_{10} P_c = c N_p N_n I + d, \tag{33}$$

where c and d are the adjustable parameters by fitting to Figs. 3 and 4 whose RSS value is minimum and coefficient

of determination $R^2 \approx 1$. The plots of the dependence for the P_c in logarithmic form with $N_p N_n I$ have been presented in Figs. 3 and 4. From these two figures, the linear correlations of the deduced cluster radioactivity preformation probability in logarithmic form with the valence nucleons (holes) numbers become more distinct when they are plotted as a function of $N_p N_n I$. It is clearly to see that cluster radioactivity preformation probability in logarithmic form are proportional to the products of effective numbers of valence particles (holes) $N_p N_n$ as well as the multiplication of the isospin asymmetry with this product $N_p N_n I$.

For further investigating the preformation mechanics for cluster radioactivity, we also compare the P_c results extracted from the experimental decay energy and half-life as well as the results obtained by using the parent-mass-number dependence analytical formula and model proposed by Wei and Zhang [42] with our work. The calculated results are well listed in Table II. In this table, the first three columns are the same as Table I. The fourth to seventh columns are shown the cluster radioactivity preformation probability in logarithmic form obtained by using CFM, UFM, Wei's model as well as Wei's formula denoted as CFM, UFM, WZM, and WZF, respectively. It is obvious to find that the general tendencies of the preformation probability in logarithmic form are similar to the pattern for the variations of P_c observed from Table I. For a more deeper insight into this phenomenon, the tendency of the variations for P_c in logarithmic form obtained by using CFM, UFM, Wei's model, and Wei's formula has been plotted in Fig. 5. From this figure, it is easy to see that the values of P_c are generally decreasing with an increasing of the mass number parent nuclei as well as the emitted cluster. For neutrons, pairing is more influential than protons

TABLE II. Cluster radioactivity preformation probability in different formulas and models. See text for details.

| decay	Q_c(MeV)	$T_{1/2}^{\exp}$	CFM	UFM	WZM	WZF
^{221}Fr $\rightarrow$ ^{207}Tl + ^{14}C	31.29	14.56	-3.204	-6.420	-10.00	-10.18
^{221}Ra $\rightarrow$ ^{207}Pb + ^{14}C	32.40	13.39	-3.126	-6.388	-9.95	-10.18
^{222}Ra $\rightarrow$ ^{208}Pb + ^{14}C	33.05	11.22	-3.037	-5.547	-8.98	-10.94
^{223}Ra $\rightarrow$ ^{209}Pb + ^{14}C	31.83	15.05	-3.440	-7.160	-10.68	-11.68
^{224}Ra $\rightarrow$ ^{210}Pb + ^{14}C	30.53	15.87	-3.186	-5.593	-9.06	-12.39
^{226}Ra $\rightarrow$ ^{212}Pb + ^{14}C	28.20	21.20	-3.211	-6.014	-9.52	-13.75
^{223}Ac $\rightarrow$ ^{209}Bi + ^{14}C	33.06	12.60	-3.341	-6.060	-9.55	-11.68
^{228}Th $\rightarrow$ ^{208}Pb + ^{20}O	44.72	20.73	-4.670	-8.174	-12.76	-15.02
^{231}Pa $\rightarrow$ ^{208}Pb + ^{23}F	51.88	26.02	-5.999	-12.495	-17.60	-16.76
^{230}Th $\rightarrow$ ^{206}Hg + ^{24}Ne	57.76	24.63	-5.661	-11.349	-16.62	-16.20
^{231}Pa $\rightarrow$ ^{207}Tl + ^{24}Ne	60.41	22.89	-6.271	-12.074	-17.50	-16.76
^{232}U $\rightarrow$ ^{208}Pb + ^{24}Ne	62.31	20.39	-5.924	-11.195	-16.43	-17.30
^{233}U $\rightarrow$ ^{209}Pb + ^{24}Ne	60.49	24.84	-6.672	-13.145	-18.44	-17.82
^{234}U $\rightarrow$ ^{210}Pb + ^{24}Ne	58.82	25.93	-6.313	-11.904	-17.18	-18.32
^{233}U $\rightarrow$ ^{208}Pb + ^{25}Ne	60.70	24.84	-6.962	-13.126	-18.56	-17.82
^{234}U $\rightarrow$ ^{208}Pb + ^{26}Ne	59.41	25.93	-6.862	-12.074	-17.65	-18.32
^{234}U $\rightarrow$ ^{206}Hg + ^{28}Mg	74.11	25.53	-7.411	-13.928	-19.82	-18.32
^{236}Pu $\rightarrow$ ^{208}Pb + ^{28}Mg	79.67	21.52	-7.689	-14.132	-19.98	-19.26
^{238}Pu $\rightarrow$ ^{210}Pb + ^{28}Mg	75.91	25.70	-7.547	-13.903	-19.80	-20.13
^{238}Pu $\rightarrow$ ^{208}Pb + ^{30}Mg	76.79	25.70	-9.452	-14.561	-20.72	-20.13
^{238}Pu $\rightarrow$ ^{206}Hg + ^{32}Si	91.19	25.28	-11.039	-15.625	-22.09	-20.13
^{242}Cm $\rightarrow$ ^{208}Pb + ^{34}Si	96.54	23.15	-11.366	-16.511	-23.20	-21.64
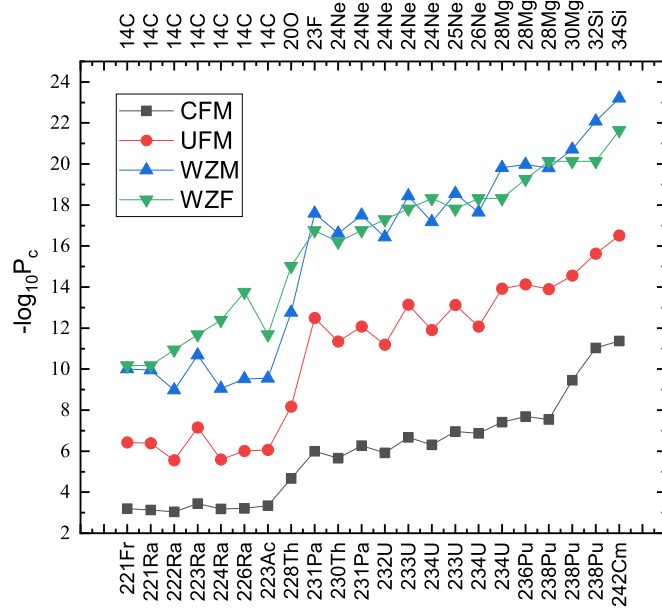
FIG. 5. The tendency of the negative values for cluster radioactivity preformation probability obtained by using different models and formulas extracted from Table II in logarithmic form.

in cluster radioactivity and most of the cluster emitters as well as the emitted cluster are neutron-rich nuclides, it is less possible for the cluster to be formed in the parent nuclei in trans-lead region far away from neutron shell closure at 126 [41].

The results of our work further validate that cluster radioactivity is closely to the nuclear shell effect. Investigation for the cluster radioactivity preformation probability explored in the scheme of $N_p N_n$ could well simply reflect the shell effects of nuclear structure and can be easily acquired as they are parametrized in the simplified functions of N_p and N_n. We hope this study could be useful for studying cluster radioactivity and further probing the nuclear structure in the trans-lead region.

IV. SUMMARY

In summary, we systematically investigate the dependence of cluster radioactivity preformation probability versus valence protons and neutrons both microscopically and model-dependently. In the microscopic approach, based on our previous work, the cluster radioactivity preformation probability is dealt with a cluster formation model (CFM) combined with the exponential relationship of P_c to the α decay preformation probability P_α when the number of the emitted cluster $A_c \leqslant 28$. Whereas $A_c \geqslant 28$, P_c is obtained through the charge-number dependence of P_c on the decay products proposed by Ren et al. In the model-dependent approach, P_c is extracted through the ratios from the calculated cluster radioactivity half-lives to experimental ones, while the cluster radioactivity half-lives are obtained within the framework of UFM. Both of the results have shown that the cluster radioactivity preformation probability P_c in the logarithmic form is proportional to the products of the valence protons and neutrons as well as the multiplication of this product with the isospin asymmetry. We also compare the results obtained by using the parent-mass-number dependence analytical formula as well as the model proposed by Wei and Zhang with our work and make a discussion about preformation mechanic for cluster radioactivity.

[1] A. Săndulescu, J. Phys. G: Nucl. Part. Phys. **15**, 529 (1989).

[2] R. K. Gupta and W. Greiner, Int. J. Mod. Phys. E **3**, 335 (1994).

[3] D. N. Poenaru and W. Greiner, J. Phys. G: Nucl. Part. Phys. **17**, S443 (1991).

[4] A. Săndulescu, D. N. Poenaru, and W. Greiner, Sov. J. Part. Nucl. **11**, 528 (1980).

[5] M. Horoi, J. Phys. G: Nucl. Part. Phys. **30**, 945 (2004).

[6] H. J. Rose and G. A. Jones, Nature (London) **307**, 245 (1984).

[7] O. A. P. Tavares and E. L. Medeiros, Phys. Scr. **86**, 015201 (2012).

[8] K. P. Santhosh and R. K. Biju, Ann. Phys. (NY) **334**, 280 (2013).

[9] M. Balasubramaniam, S. Kumarasamy, N. Arunachalam, and R. K. Gupta, Phys. Rev. C **70**, 017301 (2004).

[10] Y. L. Zhang and Y. Z. Wang, Phys. Rev. C **97**, 014318 (2018).

[11] H. G. de Carvalho, J. B. Martins, and O. A. P. Tavares, Phys. Rev. C **34**, 2261 (1986).

[12] O. A. P. Tavares and E. L. Medeiros, Eur. Phys. J. A **49**, 6 (2013).

[13] D. N. Poenaru, R. A. Gherghescu, and W. Greiner, Phys. Rev. C **83**, 014601 (2011).

[14] J. L. Chen, J. Y. Xu, J. G. Deng, X. H. Li, B. He, and P. C. Chu, Eur. Phys. J. A **55**, 214 (2019).

[15] M. Ismail, W. Seif, A. Adel, and A. Abdurrahman, Nucl. Phys. A **958**, 202 (2017).

[16] D. X. Zhu, H. M. Liu, Y. Y. Xu, Y. T. Zou, X. J. Wu, P. C. Chu, and X. H. Li, Chin. Phys. C **46**, 044106 (2022).

[17] C. Qi, F. R. Xu, R. J. Liotta, M. Y. Zhang, C. Asawatangtrakuldee, and D. Hu, Phys. Rev. C **80**, 044326 (2009).

[18] S. Luo, Y. Y. Xu, D. X. Zhu, B. He, P. C. Chu, and X. H. Li, Eur. Phys. J. A **58**, 244 (2022).

[19] D. M. Zhang, L. J. Qi, D. X. Zhu, Y. Y. Xu, S. Luo, and X. H. Li, Nucl. Sci. Tech. **34**, 55 (2023).

[20] D. X. Zhu, M. Li, Y. Y. Xu, X. J. Wu, B. He, and X. H. Li, Nucl. Sci. Tech. **33**, 122 (2022).

[21] Y. Y. Xu, H. M. Liu, D. X. Zhu, X. P, Y. T. Zou, X. H. Li and P. C. Chu, Eur. Phys. J. A **58**, 16 (2022).

[22] Y. Y. Xu, X. X. Hu, D. X. Zhu, X. J. Wu, P. C. Chu, and X. H. Li, Nucl. Sci. Tech. **34**, 30 (2023).

[23] Y. T. Zou, X. Pan, H. M. liu, X. J. Wu, B. He, and X. H. Li, Phys. Scr. **96**, 075301 (2021).

[24] H. M. Liu, Y. T. Zou, X. Pan, X. J. Bao, and X. H. Li, Chin. Phys. C **44**, 094106 (2020).

[25] X. J. Bao, H. F. Zhang, B. S. Hu, G. Royer, and J. Q. Li, J. Phys. G: Nucl. Part. Phys. **39**, 095103 (2012).

[26] M. Balasubramaniam and N. S. Rajeswari, Int. J. Mod. Phys. E **23**, 1450018 (2014).

[27] R. Kumar and M. K. Sharma, Phys. Rev. C **85**, 054612 (2012).

[28] K. P. Santhosh and T. A. Jose, Nucl. Phys. A **992**, 121626 (2019).

[29] H. M. Liu, Y. T. Zou, X. Pan, X. H. Li, X. J. Wu, and B. He, Phys. Scr. **96**, 125322 (2021).

[30] V. Dehghani, S. A. AlaviA. Soylu, and F. Koyuncu, Chin. Phys. C **46**, 044104 (2022).

[31] A. Zdeb, M. Warda, and N. Pomorski, Phys. Rev. C **87**, 024308 (2013).

[32] G. Royer and R. Moustabchir, Nucl. Phys. A **683**, 182 (2001).

[33] Z. Z. Ren, C. Xu, and Z. J. Wang, Phys. Rev. C **70**, 034304 (2004).

[34] D. D. Ni, Z. Z. Ren, T. K. Dong, and C. Xu, Phys. Rev. C **78**, 044310 (2008).

[35] R. Kumar, Phys. Rev. C **86**, 044612 (2012).

[36] D. N. Poenaru, M. Ivaşcu, A. Săndulescu, and W. Greiner, Phys. Rev. C **32**, 572 (1985).

[37] Y. Z. Wang, F. Z. Xing, Y. Xiao, and J. Z. Gu, Chin. Phys. C **45**, 044111 (2021).

[38] K. P. Santhosh, R. K. Biju, and A. Joseph, J. Phys. G: Nucl. Part. Phys. **35**, 085102 (2008).

[39] K. Prathapan, M. K. Preethi Rajan, and R. K. Biju, Int. J. Mod. Phys. E **31**, 2250068 (2022).

[40] L. J. Qi, D. M. Zhang, S. Luo, X. H. Li, C. T. Liang, and X. J. Wu, Chin. Phys. C **47**, 014101 (2023).

[41] M. Ismail, A. Y. Ellithi, M. M. Selim, N. Abou-Samra, and O. A. Mohamedien, Phys. Scr. **95**, 075303 (2020).

[42] K. Wei and H. F. Zhang, Phys. Rev. C **96**, 021601(R) (2017).

[43] S. S. Malik and Raj K. Gupta, Phys. Rev. C **39**, 1992 (1989).

[44] K. Wei and H. F. Zhang, Phys. Rev. C **102**, 034318 (2020).

[45] M. Bhattacharya, S. Roy, and G. Gangopadhyay, Phys. Lett. B **665**, 182 (2008).

[46] G. Gangopadhyay, J. Phys. G: Nucl. Part. Phys. **36**, 095105 (2009).

[47] J. M. Dong, H. F. Zhang, J. Q. Li, and W. Scheid, Eur. Phys. J. A **41**, 197 (2009).

[48] G. L. Zhang, Y. J. Yao, M. F. Guo, M. Pan, G. X. Zhang, and X. X. Liu, Nucl. Phys. A **951**, 86 (2016).

[49] F. Saidi, M. R. Oudih, M. Fellah, and N. H. Allal, Mod. Phys. Lett. A **30**, 1550150 (2015).

[50] F. G. Kondev, M. Wang, W. J. Huang, S. Naimi, and G. Audi, Chin. Phys. C **45**, 030001 (2021).

[51] M. Wang, W. J. Huang, F. G. Kondev, G. Audi, and S. Naimi, Chin. Phys. C **45**, 030003 (2021).

[52] D. D. Ni and Z. Z. Ren, Phys. Rev. C **82**, 024311 (2010).

[53] J. G. Deng, J. C. Zhao, P. C. Chu, and X. H. Li, Phys. Rev. C **97**, 044322 (2018).

[54] S. M Saleh Ahmed, R. Yahaya, S. Radiman, and M. S. Yasir, J. Phys. G: Nucl. Part. Phys. **40**, 065105 (2013).

[55] S. M. S. Ahmed, Nucl. Phys. A **962**, 103 (2017).

[56] D. M. Deng, Z. Z. Ren, D. D. Ni, and Y. B. Qian, J. Phys. G: Nucl. Part. Phys. **42**, 075106 (2015).

[57] D. M. Deng and Z. Z. Ren, Phys. Rev. C **93**, 044326 (2016).

[58] R. Blendowske and H. Walliser, Phys. Rev. Lett. **61**, 1930 (1988).

[59] W. M. Seif, M. Shalaby, and M. F. Alrakshy, Phys. Rev. C **84**, 064608 (2011).

[60] W. Seif, J. Phys. G: Nucl. Part. Phys. **40**, 105102 (2013).

[61] X. D. Sun, P. Guo, and X. H. Li, Phys. Rev. C **94**, 024338 (2016).

[62] J. G. Deng, J. C. Zhao, D. Xiang, and X. H. Li, Phys. Rev. C **96**, 024318 (2017).